Journal of Thermal Analysis, Vol. 50 (1997) 625-632

THERMAL DECOMPOSITION OF THE MAGNESIUM, ZINC, LEAD AND NIOBIUM CHELATES DERIVED FROM 8-QUINOLINOL

*S. A. Juiz, M. I. G. Leles, A. C. F. Caires, N. Boralle and M. Ionashiro**

Instituto de Química, UNESP, Araraquara, São Paulo, C. P. 355, CEP 14800–900, Brazil

(Received January 4, 1996; in revised form October 26, 1996)

Abstract

Solid M-Ox compounds, where *M* represents Mg(II), Zn(II), Pb(II) and NbO(III), and Ox is 8-quinolinol, have been prepared. Thermogravimetry, derivative thermogravimetry (TG, DTG), differential scanning calorimetry (DSC), nuclear magnetic resonance (NMR) and infrared absorption spectra (IR) have been used to characterize and to study the thermal stability and thermal decomposition of these compounds.

Keywords: DSC, NMR, 8-quinolinol compounds, TG-DTG, stability, thermal decomposition

Introduction

Several investigations have been carried out on the dehydration and thermal behaviour of some metal chelates of 8-quinolinol in static air atmosphere [1–6]; in vacuo [7]; in dynamic argon atmosphere [8–13] and in dynamic nitrogen atmosphere [14].

In the present work the thermal stability and thermal decomposition of Mg(II), Zn(II), Pb(II) and NbO(III) chelates of 8-quinolinol were investigated by TG, DTG and DSC in a dynamic air atmosphere and NMR and IR spectra were applied to characterize the product of thermal decomposition.

Experimental

Aqueous solutions of metal ions were mixed with a slight excess of a 5% solution of 8-quinolinol in 12% acetic acid and subsequent neutralization with a solution of ammonium hydroxide. The aqueous solution of niobium ions was pre-

* Author to whom all correspondence should be addressed.

0368–4466/97/ $ 5.00

John Wiley & Sons Limited
Chichester

pared by dissolving Nb_2O_5 with hydrofluoric acid solution. The precipitates were collected on a Büchner filter, washed thoroughly with hot water to remove any excess 8-quinolinol and then air-dried for 25 h at room temperature and stored in a desiccator over anhydrous calcium chloride.

TG, DTG and DSC curves were obtained using a Mettler TA-4000 thermoanalyser system with an air flux of >150 ml min^{-1}, a heating rate of 10 K min^{-1} and with samples weighing about 7 mg. An alumina crucible was used in the TG and DTG studies and an aluminium crucible was used in the DSC measurements.

Nuclear magnetic resonance unidimensional (^1H, ^{13}C and DEPT135) and bidimensional (COSY and CHCORR) spectra were recorded on a Bruker A.C.-200, multi-nuclear spectrometer in DMSO-d6 solution with tetramethyl silane as internal standard. Infrared spectra were recorded on a Nicolet Impact-400 instrument with a resolution of 4 cm^{-1} by using a liquid film technique in $CHCL_3$.

Results and discussion

Table 1 presents the thermoanalytical (TG) results of the prepared compounds with compositions represented by the formula $ML_2 \cdot 2H_2O$ (M=Mg, Zn); PbL_2 and $NbOL_3$ (L=8-quinolinol).

The TG, DTG and DSC curves are shown in Figs 1 and 2, respectively. For the magnesium compound the TG and DTG curves in Fig. 1(a), show mass losses in two steps, and the DSC curve in Fig. 2(a) shows an endothermic peak and an exothermic process with evidence of several consecutive phenomena. The first mass loss up to 453 K, corresponding to the endothermic peak at 443 K, is due to the dehydration with loss of $2H_2O$. The second mass loss between 713 and 843 K is ascribed to the thermal decomposition of the anhydrous compound with formation of magnesium oxide, MgO. In this step, the DSC curve shows a sequence of endothermic and exothermic peaks attributed to crystalline transition (713 K), partial oxidation accompanied by evaporation of the ligand (753, 773 K) and final pyrolysis of the carbonaceous residue (793 K). The fusion of the compound (733 K) is in disagreement with data in [9], probably due to the exothermic process at 713 K, which may provoke a premature fusion of the compound.

Table 1 Thermoanalytical (TG) results

Compound	Metal/%		*L*/%		Water/%	
	Theor.	TG	Theor.	TG	Theor.	TG
$Mg(Ox)_2 \cdot 2H_2O$	6.97	7.01	78.10	77.57	10.34	10.79
$Zn(Ox)_2 \cdot 2H_2O$	16.77	16.32	69.87	70.41	9.25	9.29
$Pb(Ox)_2$	41.81	41.61	54.96	55.18		
$NbO(Ox)_3$	17.16	17.24	75.45	75.29		

Ox means 8-quinolinol

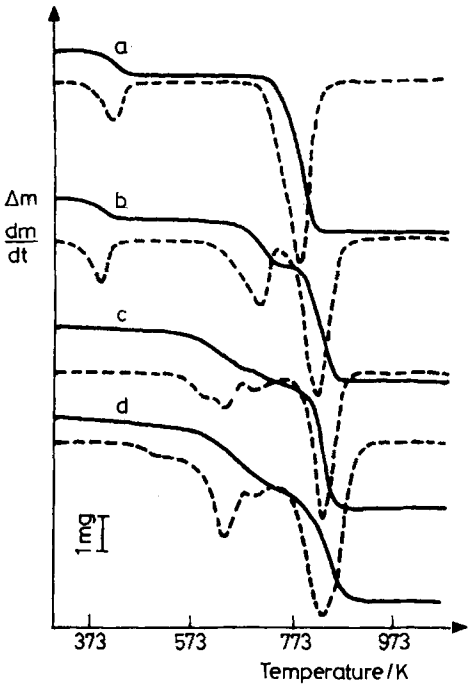

Fig. 1 TG, DTG curves of the compounds: a) $Mg(Ox)_2 \cdot 2H_2O$ (7.780 mg); b) $Zn(Ox)_2 \cdot 2H_2O$ (7.370 mg); c) $Pb(Ox)_2$ (7.023 mg) and d) $NbO(Ox)_3$ (7.116 mg)

For the zinc compound the TG and DTG curves in Fig. 1(b) show mass losses in three steps, and the DSC curve in Fig. 2(b), shows three endothermic and two exothermic peaks and a further exothermic process. The first mass loss up to 423 K, corresponding the endothermic peak at 413 K is due to dehydration with loss of $2H_2O$. The second mass loss between 623 and 733 K, corresponding to the exothermic and endothermic peaks at 683 and 693 K is attributed to the almost simultaneous partial oxidation and evaporation of the ligand. The third mass loss between 733 and 873 K, corresponding to the exothermic process between 713 K and >873 K is due to the final pyrolysis of the ligand, with formation of zinc oxide, ZnO. The exothermic peak at 468 K is ascribed to the recrystallization of the compound that occurs after the dehydration. The sharp endothermic peak at 623 K is due to the fusion of the anhydrous compound and it is in agreement with data in [9].

For the lead compound obtained in the anhydrous form, the TG and DTG curves in Fig. 1(c) show mass losses in three consecutive steps, and the DSC curves in Fig. 2(c) show a sequence of endothermic and exothermic peak and a further exothermic process. The first and second mass losses between 553 and 743 K are due to the almost simultaneous partial oxidation and evaporation of the ligand. The last mass loss between 743 and 893 K, corresponding to the exo-

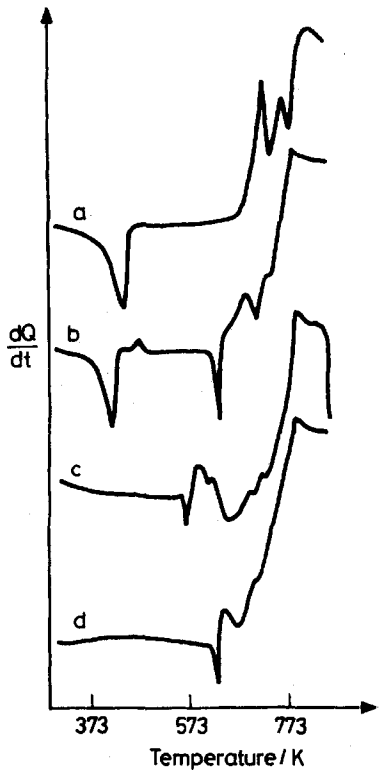

Fig. 2 DSC curves of the compounds: a) $Mg(Ox)_2 \cdot 2H_2O$ (7.708 mg); b) $Zn(Ox)_2 \cdot 2H_2O$ (6.673 mg); c) $Pb(Ox)_2$ (7.510 mg) and d) $NbO(Ox)_3$ (6.305 mg)

thermic trace between 743 K and >873 K, is due to the final pyrolysis of the ligand with formation of lead oxide, PbO. The endothermic peak at 568 K is due to the fusion of the compound and it is in disagreement with [9].

For the niobium compound, not yet reported in the literature, which was obtained in the anhydrous form, the TG and DTG curves, in Fig. 1(d) show mass losses in two (TG) and four (DTG) consecutive steps. The mass loss up to 723 K, corresponding to the exothermic and endothermic peaks at 653 and 673 K respectively, is attributed to the almost simultaneous partial oxidation and evaporation of the ligand. The mass loss between 723 and 913 K, corresponding to the exothermic process between 683 K and >873 K is due to the final pyrolysis of the carbonaceous residue with formation of niobium oxide, Nb_2O_5. The sharp endothermic peak at 633 K is due to the fusion of the compound.

The interpretation of the DSC curves of the anhydrous compounds does not agree with literature data, because the atmospheres used were not the same.

Interpretation of the thermal decomposition of the anhydrous compounds was based on experiments made with samples heated in a long test tube under approximately the same conditions as the TG and DSC curves. In these experi-

ments, fusion and carbonaceous residue were observed. Deposits of a mixture of white and yellow solids on the cool part of the test tube were also observed (more white material for the magnesium and more yellow material for the other compounds), corresponding to the first mass loss of the anhydrous compound observed in the TG and DTG curves, except for the magnesium compound where the evaporation and pyrolysis of the carbonaceous residue occur simultaneously.

The white solid was identified as hydrated quinoline N-oxide (*m.p.*=325–328 K, observed; 324–328 K, literature). The structure of the yellow solid (*m.p.*=616–621 K, observed; not found in the literature), was elucidated by nuclear magnetic resonance (carbon 13, DEPT, COSY and CHCORR). The assignment of values of chemical shifts of ^{1}H and ^{13}C was carried out by comparison with literature data and by spectral analysis and empirical calculations for the values of chemical shifts of ^{13}C.

By analysis of proton spectra, and comparison with 8-quinolinol, it was possible to identify the protons of the pyridine ring (Table 2). The bidimensional homonuclear spectrum of protons (COSY) shows interactions between protons 2 (8.67 ppm) and 3 (7.54 ppm) and at long range with proton 4 (8.37 ppm). Interactions between proton 4 (8.37 ppm) and proton 2 (8.67 ppm) are also observed, helping in the assignments of values of chemical shifts of the protons in the pyridine ring (Table 3).

Table 2 Values of chemical shifts of proton in 200 MHz NMR (DMSO-d_6)

H	ppm	m	J(Hz)
2	8.67	d	3.5
3	7.54	dd	8.0
4	8.37	d	8.0
6	6.93	d	8.0
7	7.36	dd	8.0
8	6.84	d	8.0

Table 3 Correlations in bidimensional homonuclear COSY spectrum in 200 MHz (DMSO-d_6)

H	ppm	m	J(Hz)
2	8.67	3	7.54
		4	8.37s
4	8.37	2	8.67s
		3	7.54
7	7.36	6	6.93

s=small

The assignments of values of chemical shifts of carbon were established by ^{13}C NMR data and direct ^{1}H-^{13}C correlations in bidimensional spectra CHCORR besides the DEPT spectra that make evident the multiplicity of the carbon signals observed.

The assignment by ^{13}C (Table 4) was realized by comparison with models previously described in the literature for quinoline [14] and quinoline N-oxide besides empirical calcules [15].

Table 4 Values of chemical shifts of the carbons in 50 MHz NMR and multiplicity by DEPT spectra (DMSO-d_6)

C	ppm	m
2	145.4	CH
3	121.6	CH
4	138.8	CH
4a	129.5	q
5	161.8	q
6	109.8	CH
7	130.0	CH
8	112.2	CH
8a	139.8	q

The DEPT 135 and CHCORR spectra help in the assignment, since the first give us information about the absence of CH2 groups and the presence of six CH groups and three quaternary carbons (Table 4), whereas the bidimensional spectra CHCORR showed correlation between carbon at 145.4, 138.8, 121.6 and 112.2 ppm, with protons at 8.67 (H-2), 8.37 (H-4), 7.54 (H-3) and 6.84 ppm (H-8) which permits attribution of these values to carbon 2, 4, 3 and 8, respectively.

The infrared spectrum shows a strong absorption band at 1393 cm^{-1} characteristic of nitroso compounds, as well as a sharp band at 3387 cm^{-1} characteristic of the stretching of hydroxyl groups in compounds containing polymeric association [16]. The absence of carbonyl groups indicates that the oxidation occurs at the nitrogen.

The data of NMR, IR and mp permit the suggestion that the yellow solid is 5-quinolinol N-oxide.

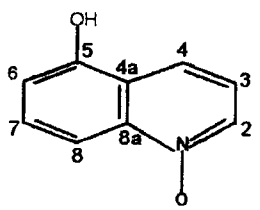

Calculations based on the mass losses observed in the TG curves as well as information obtained from DSC curves, NMR, IR spectra and mp permit us to propose the following thermal decomposition mechanisms:

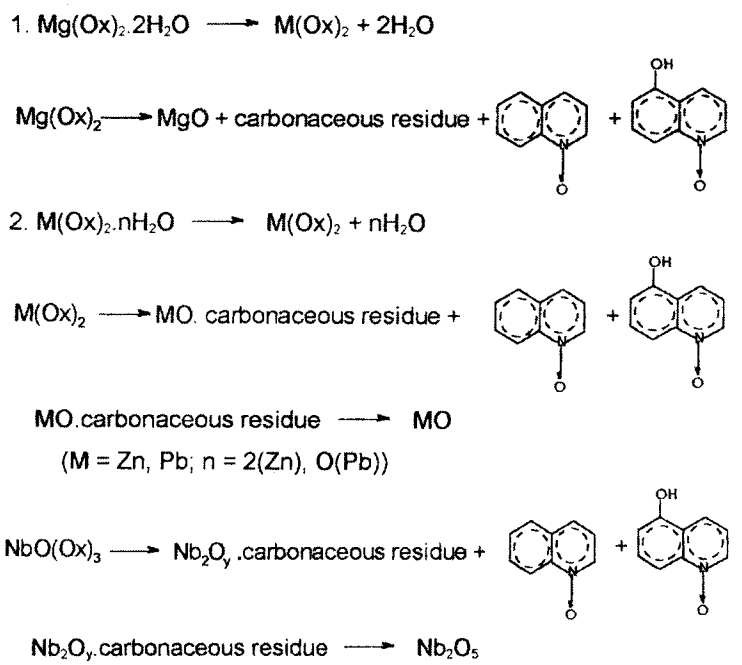

Conclusions

The TG, DTG and DSC curves obtained under an air flux provided previously unreported information about the thermal decomposition of these compounds.

The NMR, IR and mp data also provided information about the white and yellow solids obtained as thermal decomposition products.

* * *

The authors acknowledge the FAPESP (Proc. 90/2932-4), CAPES and CNPq for financial support.

References

1 S. Peltier and C. Duval, Anal. Chim. Acta, 1 (1947) 345.
2 Th. Duval and C. Duval, Anal. Chim. Acta, 2 (1948) 50.
3 Th. Dupuis and C. Duval, Anal. Chim. Acta, 3 (1949) 203.
4 Th. Dupuis, J. Besson and C. Duval, Anal. Chim. Acta, 3 (1949) 603.
5 M. Borrel and R. Pâris, Anal. Chim. Acta, 4 (1950) 267.
6 M. Borrel and R. Pâris, Anal. Chim. Acta, 5 (1951) 573.

7 R. G. Charles and A. Langer, J. Phys. Chem., 63 (1959) 603.
8 R. G. Charles, J. Inorg. Nucl. Chem., 20 (1961) 211.
9 R. G. Charles, Anal. Chim. Acta, 27 (1962) 474.
10 W. W. Wendlandt and R. Horton, Anal. Chem., 34 (1962) 1098.
11 R. G. Charles, A. Perrotto and M. A. Dolan, J. Inorg. Nucl. Chem., 25 (1963) 45.
12 R. G. Charles and A. Perrotto, Anal. Chim. Acta, 30 (1964) 131.
13 R. G. Charles, Anal. Chim. Acta, 31 (1964) 405.
14 R. H. Gore and W. W. Wendlandt, Anal. Chim. Acta, 52 (1970) 83.
15 H. O. Kalinowsky, S. Berger and S. Braun, Carbon 13 NMR Spectroscopy, John Wiley & Sons, 1988, p. 392.
16 E. Breitmaier and W. Voelter, Carbon-13 Spectroscopy, Weinheim, New York 1987, p. 289, 319.
17 J. R. Dyer, Aplicações de Espectroscopia de Absorção aos Compostos Orgânicos, Ed. Edgard Bücher, 1962, p. 33, 39.